Hydrologic Impacts of Surface Elevation and Spatial Resolution in Statistical Correction Approaches: Case Study of Flumendosa Basin, Italy

Enrica Perra, Ph.D.[1]; Francesco Viola, Ph.D.[2]; Roberto Deidda[3]; Domenico Caracciolo, Ph.D.[4]; Claudio Paniconi[5]; and Andreas Langousis, Sc.D., P.E., M.ASCE[6]

Abstract: The role of surface elevation and spatial resolution in statistical correction approaches for temperature and precipitation forcing is investigated using four global climate model (GCM) and regional climate model (RCM) combinations. A Mediterranean basin characterized by steep orography and prone to extreme flooding is chosen as a test case. For this aim, precipitation is statistically downscaled using a parametric scheme for bias correction and high-resolution downscaling and a widely used nonparametric approach, with nominal resolution equal to that of the GCM/RCM. Temperature fields are reprojected from climate model to terrain elevation at high resolution. The response of the basin in terms of discharge, actual evapotranspiration, and leakage is simulated using the TOPographic Kinematic APproximation and Integration (TOPKAPI-X) model from 1951 to 2099 and at multiple spatial scales. To investigate the role of orography, simulations are run applying the downscaling schemes on a flat terrain. The results show that, independently of the size of the basin, the elevation factor minimally affects the simulated hydrological response, whereas the effect of the spatial resolution of downscaled precipitation fields on the hydrological budget components is significant, and depends on the catchment size. **DOI: 10.1061/(ASCE)HE.1943-5584.0001969.** *This work is made available under the terms of the Creative Commons Attribution 4.0 International license, https://creativecommons.org/licenses/by/4.0/.*

Author keywords: Surface elevation; Spatial resolution; Statistical correction approaches; Mediterranean region; Climate models; (TOPographic Kinematic APproximation and Integration) TOPKAPI-X.

Introduction

Studies regarding the hydrological signature of climate change have become increasingly important in recent decades, as climate-related extremes (in the form of heat waves, droughts, floods, cyclones, wildfires, etc.) have impacted natural and human systems, revealing their significant exposure and vulnerability to climatic variations (e.g., Stahl et al. 2011; Casper et al. 2012; IPCC 2014; Mendoza et al. 2014; Teutschbein et al. 2015). Hence, understanding the Earth's atmospheric response to natural and anthropogenic forcings takes on primary importance when developing climate change adaptation strategies (e.g., Wilby 2010; Langousis et al. 2016; Mamalakis et al. 2017).

GCMs and RCMs are numerical algorithms capable of simulating the past, present, and future of Earth's climate under various natural and anthropogenic forcings, including different greenhouse gas emission scenarios (e.g., Vrac et al. 2007; Raje and Mujumdar 2009; Wetterhall et al. 2009; Deidda et al. 2013; Langousis and Kaleris 2014). GCMs capture the main features of atmospheric circulation at synoptic scales, with nominal resolution of a few degrees of longitude and latitude (e.g., von Storch et al. 1993; Prudhomme et al. 2002; Déqué 2007; Palatella et al. 2010), while RCMs improve on the GCM accuracy by resolving atmospheric and hydrological processes on a finer computational grid (i.e., on the order of a quarter of a degree) over a limited domain, nested within the coarser grid of the GCM (e.g., Giorgi et al. 2001; Salathé 2003; Fowler et al. 2007; Maraun et al. 2010; Rummukainen 2010; Teutschbein and Seibert 2013). However, as demonstrated by a number of studies (e.g., Mearns et al. 1995; Walsh and McGregor 1995; Bates et al. 1998; Charles et al. 1999; Busuioc et al. 2006; Kiktev et al. 2007; Dibike et al. 2008; Baguis et al. 2010; Smiatek et al. 2009; Urrutia and Vuille 2009; Kjellström et al. 2010; Gagnon and Rousseau 2014; Hasson et al. 2013; Mamalakis et al. 2017), precipitation is the less well-reproduced variable by GCMs and RCMs, with raw climate model products demonstrating limited success in reproducing the intensity and frequency of daily precipitation, the distribution of the durations of dry and wet periods, and the distribution of rainfall extremes.

[1]Dipartimento di Ingegneria Civile, Ambientale ed Architettura, Università degli Studi di Cagliari, Cagliari 09122, Italy (corresponding author). ORCID: https://orcid.org/0000-0002-1315-125X. Email: enrica.perra@unica.it

[2]Associate Professor, Dipartimento di Ingegneria Civile, Ambientale ed Architettura, Università degli Studi di Cagliari, Cagliari 09122, Italy. Email: viola@unica.it

[3]Professor, Dipartimento di Ingegneria Civile, Ambientale ed Architettura, Università degli Studi di Cagliari, Cagliari 09122, Italy. Email: rdeidda@unica.it

[4]Regional Environmental Protection Agency of Sardinia, Via Biasi 7, Cagliari 09122, Italy. ORCID: https://orcid.org/0000-0003-2381-0025. Email: dcaracciolo@arpa.sardegna.it

[5]Professor, Centre Eau Terre Environnement, Institut National de la Recherche Scientifique, Quebec, Canada G1K9A9. Email: claudio.paniconi@ete.inrs.ca

[6]Associate Professor, Dept. of Civil Engineering, Univ. of Patras, Patras 26504, Greece; Professeur Associé, Centre Eau Terre Environnement, Institut National de la Recherche Scientifique, Quebec, Canada G1K9A9. ORCID: https://orcid.org/0000-0002-0643-2520. Email: andlag@alum.mit.edu

Note. This manuscript was submitted on July 24, 2019; approved on April 7, 2020; published online on July 14, 2020. Discussion period open until December 14, 2020; separate discussions must be submitted for individual papers. This paper is part of the ***Journal of Hydrologic Engineering***, © ASCE, ISSN 1084-0699.

Because rainfall constitutes the main source of water in a catchment, its accurate estimation becomes important when modeling hydrological budget components (e.g., Haddeland et al. 2002; Smith et al. 2004; Zehe et al. 2005; Das et al. 2008; Kaleris et al. 2017), evaluating climatic effects on a catchment's water balance (Sulis et al. 2011; Hagemann et al. 2013; Chang et al. 2018; Langousis et al. 2018; Perra et al. 2018; Reshmidevi et al. 2018), and assessing flood risks. To that extent, several statistical methodologies have been developed to bias correct and downscale GCM/RCM results to finer spatial scales suitable to run hydrological models and assess the availability of water resources and flood risks. The bias correction procedures encompass linear and power transformations (e.g., Durman et al. 2001; Kleinn et al. 2005; Fowler and Kilsby 2007; Leander and Buishand 2007; Lenderink et al. 2007; Leander et al. 2008; van Pelt et al. 2012) and, in the most general case, distribution mapping (e.g., Déqué 2007; Déqué et al. 2007; Piani et al. 2010; Rojas et al. 2011; Sun et al. 2011; Sulis et al. 2012; Gutmann et al. 2014; Mao et al. 2015; Mehrotra et al. 2016), with the implicit assumption (in all cases) that the correction remains invariant under time shifts (e.g., Michelangeli et al. 2009; Teutschbein and Seibert 2012, 2013). During the last 20 years, several statistical downscaling schemes have been developed to model rainfall occurrence and amount. These approaches can be classified into three broad categories: transfer functions, stochastic weather generators, and scaling or nonscaling models for stochastic rainfall simulation (see e.g., Hewitson and Crane 1996; Zorita and van Storch 1997; Wilby et al. 2004; Willems and Vrac 2011; Willems et al. 2012; Langousis and Kaleris 2014).

Generally, the choice of the most appropriate downscaling technique depends on the variables to be downscaled and their temporal and spatial resolution, as well seasonal, region, and study specific considerations (e.g., Wood et al. 2002; Maurer and Hidalgo 2008). Therefore, a large number of studies have focused on analyzing the strengths and weaknesses of different techniques in downscaling daily precipitation fields across topographically complex regions (Wilby et al. 1998; Haylock et al. 2008; Schmidli et al. 2007; Hertig and Jacobeit 2008; Tryhorn and DeGaetano 2011; Lutz et al. 2012; Jacobeit et al. 2014; Sarr et al. 2015; Sunyer et al. 2015; Langousis et al. 2016; Ochoa et al. 2016; Mamalakis et al. 2017; Gutiérrez et al. 2018), and considerable effort has been put in combining their strengths to obtain more suitable climate scenarios for basin scale hydrological applications (e.g., Wood et al. 2004; Chen et al. 2012b; Schepen et al. 2012; Vrac et al. 2012; Yoon et al. 2012; Guyennon et al. 2013).

As demonstrated by multiple studies (e.g., Wilby et al. 1999, 2000; Mearns et al. 2003; Dibike and Coulibaly 2005; Chen et al. 2013; Cannon et al. 2015; Fang et al. 2015; Gutiérrez et al. 2018), contrary to raw climate model outputs that may lead to pronounced biases, downscaled climate model results tend to produce more realistic simulations of the basin-scale hydrological processes. However, the choice of the downscaling method is not error free, because it may also lead to considerable biases and epistemic uncertainties in the simulated components of the catchment's hydrological budget (e.g., Seguí et al. 2010; Teutschbein et al. 2011; Chen et al. 2012a; Sulis et al. 2012; Nover et al. 2016; Potter et al. 2018). To that extent, several studies (e.g., Wood et al. 2004; Maurer and Hidalgo 2008; Themeßl et al. 2011; Stoll et al. 2011; Teutschbein and Seibert 2012, 2013), have indicated distribution mapping [also referred to as quantile-quantile (Q-Q) correction, histogram equalization, Q-Q mapping, etc. (see Michelangeli et al. 2009; Sennikovs and Bethers 2009; Piani et al. 2010; Sun et al. 2011; Rojas et al. 2011; Sulis et al. 2012)] as the least-sensitive bias correction approach to long-term climatic variations and, therefore, the most suitable one for hydrological applications.

In this study, our focus is on the effects of surface elevation and spatial resolution of statistical downscaling approaches in quantifying the hydrological budget components of a Mediterranean catchment prone to extreme flooding, namely the Flumedosa basin in southeast Sardinia, Italy. In doing so, we use climate model precipitation and temperature data for scenario A1B, from four GCM/RCM combinations used in the ENSEMBLES project (Hewitt and Griggs 2004)), with approximate spatial resolution of 25 km. The aforementioned GCM/RCM model combinations have been identified in the context of project CLIMB (Climate Induced Changes on the Hydrology of Mediterranean Basins, http://www.climb-fp7.eu; Ludwig et al. 2010) as the most representative ones in terms of temperature and precipitation for several catchments in the Mediterranean region, including the island of Sardinia (Deidda et al. 2013).

Statistical downscaling of precipitation is conducted using: (1) the parametric scheme of Mamalakis et al. (2017) for bias correction and high-resolution spatial downscaling (1 km); and (2) a widely used nonparametric approach based on empirically derived Q-Q correction relationships, with nominal resolution equal to that of GCM/RCM results (25 km). Temperature is interpolated in space at 1-km resolution through lapse rate corrections. In particular, we analyze the simulated hydrological response of the basin by using the aforementioned downscaled climate model outputs of precipitation and temperature considering or not the surface elevation (in the latter case by reprojecting outputs at the mean elevation of the basin).

The hydrological budget of the catchment is simulated using the extended version of the TOPKAPI (TOPographic Kinematic APproximation and Integration) model (Ciarapica and Todini 2002) during five nonoverlapping 30-year periods (i.e., 1951–1980, 1981–2010, 2011–2040, 2041–2070, and 2071–2099) and at multiple spatial scales (i.e., at the outlet of the Flumendosa basin and at 32 subcatchments).

In the section on study area and dataset, we present the Flumendosa basin and the available data used for the hydrological model calibration. In the methods section, we outline the downscaling techniques applied to disaggregate climate model outputs of precipitation and temperature, and a schematic representation of the hydrological processes modeled by the TOPKAPI-X model, with details on relevant parameterizations. A comprehensive discussion of the obtained results is presented in the section "Results," with particular emphasis on the observed differences in the simulated water budget components. Concluding remarks, important considerations, and future directions are presented in the section "Conclusions."

Study Area and Dataset

The study site is the catchment of Flumendosa located in southeast Sardinia, Italy (Fig. 1). It is one of the main basins in Sardinia, with a strategic relevance to the region's water system. It drains an area of 1,826 km^2, with elevation ranging from the highest peak of the island (1,834 m, on the Gennargentu range) to the outlet at Tyrrhenian Sea. The length of the main stream is approximately 95 km, its average slope is 36%, and its concentration time is 16 h.

The Flumendosa basin supplies water to almost all of southern Sardinia, which is the most populated area of the island. Along the Flumendosa river and its tributaries, three reservoirs have been constructed, with a total capacity of 600 mm^3, constituting the main water resource for domestic, irrigation, and industrial uses.

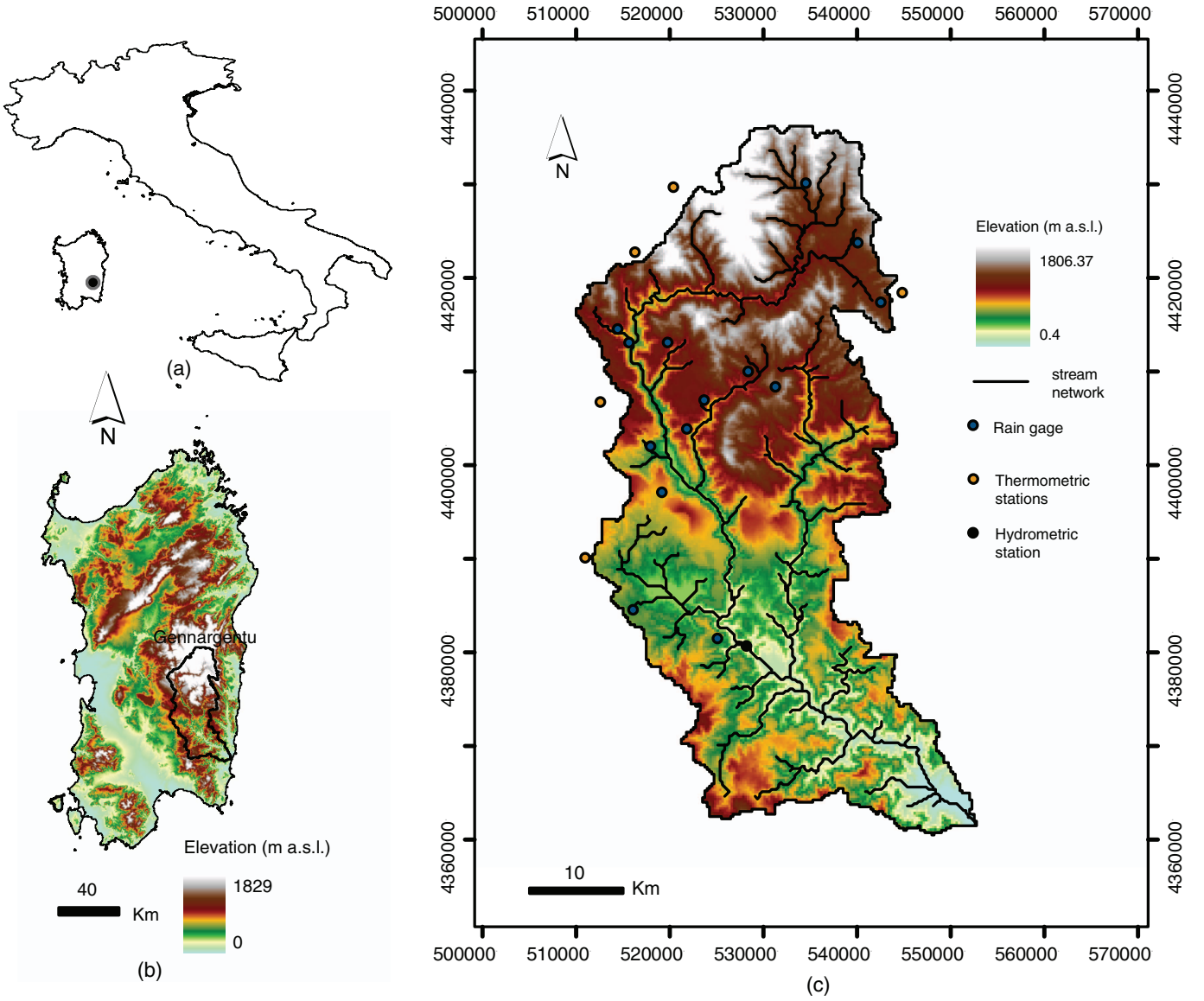

Fig. 1. (Color) Location of Flumendosa basin in (a) Italy; (b) the island of Sardinia; and (c) boundaries in WGS84 UTM coordinates, elevation, stream network, and location of hydrometeorological stations inside or near the Flumendosa basin during the period 1926–1936. (Adapted from Perra 2018.)

Southern Sardinia is prone to prolonged drought periods, which trigger social and economic problems due to conflicts among diverse water uses. In addition, some of the villages in the basin have suffered extreme flood events with important social and economic consequences, including human life losses. The complex orography, the importance for water needs, and the exposure to climatic variability in the form of both droughts and floods, make the Flumendosa basin an ideal test case for this study.

Focusing on the period before the construction of the reservoirs, daily hydrometeorological data from the Italian Hydrological Survey (the Annali Idrologici) were collected for the wider area of Flumendosa for the period 1926 to 1936, including daily precipitation measurements from 14 rain gauges, daily minimum and maximum temperatures from 5 thermometric stations, and daily discharge data from one hydrometric station [Fig. 1(c)]. Fig. 2 reports the mean monthly values of precipitation, streamflow, and temperature during the considered period. The mean annual precipitation and discharge are about 900 and 250 mm, respectively, while the mean monthly temperature ranges from 6°C in winter to 24°C in summer.

Geospatial data for the Flumendosa basin, required for the subsequent implementation and calibration of the distributed hydrological model, were provided by different agencies of the Sardinian Regional Government, and include: a digital elevation model (DEM) at 10-m resolution [Fig. 1(c)]; a pedologic map (Aru et al. 1992) with seven soil classes [Fig. 3(a)]; and a CORINE land cover (LC) map (Briggs and Martin 1988) for the year 2008 reclassified into eight groups [Fig. 3(b)]. Use of the CORINE LC map from 2008 as a reference for the 1927–1936 simulation period is justified by the fact that over the years there have been minimal long-term changes in the vegetation cover, as well as the urbanization level of the study region, i.e., the Flumendosa basin includes a natural park, major cities are located near the coast, while the villages in the inland areas are very small (about 50 inhabitants/km^2).

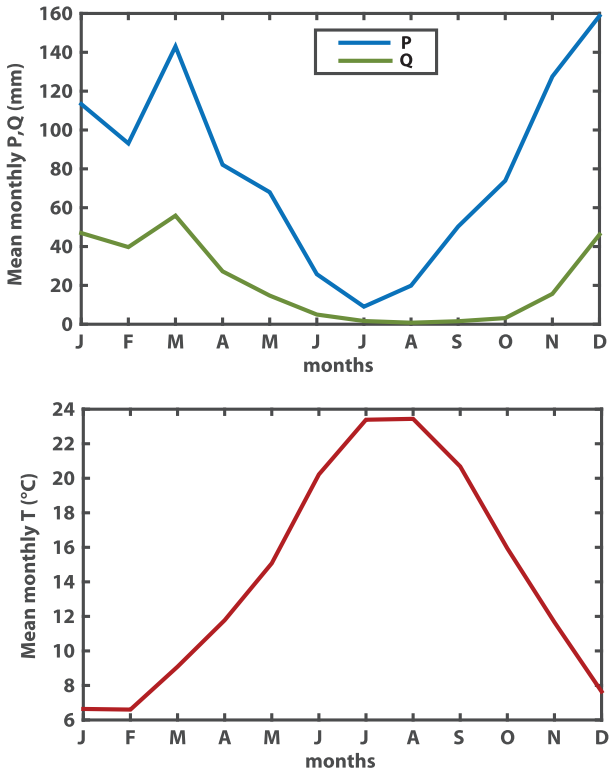

Fig. 2. (Color) Mean monthly precipitation (P), discharge (Q), and temperature (T) of Flumendosa basin during the period 1926–1936. (Adapted from Perra 2018.)

In the Flumendosa basin, 32 internal river sections were identified and are depicted in Fig. 3(c), where the Strahler stream order is also shown. The characteristics of the subcatchments in terms of area, mean elevation, slope, soil texture, and LC are reported in Table 1.

Methods

Downscaling Techniques

To study how surface elevation and the spatial resolution of statistical correction approaches affect the modeled hydrological response of the Flumendosa basin, we used an ensemble of four combinations of GCM/RCM historical runs and future projections from the ENSEMBLES project. These have been selected in the context of CLIMB project as the best-performing ones in terms of precipitation and temperature intra-annual variability in several catchments of the Mediterranean region, including the island of Sardinia (Deidda et al. 2013; Langousis et al. 2016; Mamalakis et al. 2017). More specifically, ECH-RCA, ECH-REM, and ECH-RMO combinations use the ECHAM5 (Max Planck Institute for Meteorology, Germany) GCM to drive respectively the simulations of RCA (Swedish Meteorological and Hydrological Institute), REMO (Max Planck Institute for Meteorology, Hamburg, Germany), and RACMO (Royal Netherlands Meteorological Institute) RCMs, while the combination HCH-RCA uses the output of the GCM HadCM3 (Hadley Centre for Climate Prediction, Met Office, UK) to drive the RCM RCA simulation.

The domain of integration is common to all RCMs, with a resolution of approximately 25 km. The raw climate model precipitation outputs were statistically downscaled during the period from 1951 to 2099 using: (1) the parametric statistical scheme of Mamalakis et al. (2017), referred to henceforth as PAR, that allows bias correction and high-resolution (1-km) spatial downscaling; and (2) a widely used nonparametric approach based on empirically derived Q-Q correction relationships, referred to henceforth as EMP, with resolution equal to that of the GCM/RCM results (25 km). Both downscaling approaches have been applied, compared, and tested over the whole Island of Sardinia based on multiple independent calibration and validation timeframes, using daily raingauge measurements and GCM/RCM simulations for the historical period 1951–2008 [see Mamalakis et al. (2017)]. The considered statistical downscaling approaches are conceptually equivalent, but the parametric method allows for very high spatial resolution, by fitting a two component theoretical distribution model to observational and climate model rainfall data, and interpolating the corresponding distribution parameters on a user-defined high-resolution grid, using kriging for uncertain data. The nonparametric approach does not allow for high resolution spatial downscaling, because Q-Q mapping is conducted by matching the empirical quantiles of the historical and simulated rainfall series at the spatial resolution of the RCM grid (i.e., 25 km). Interpolation in space of raw climate model temperature data was obtained by reprojection from climate model elevation to terrain elevation at 1-km resolution through local lapse rate corrections as in Caracciolo et al. (2017). The downscaled temperature values are referred to henceforth as (T).

We analyze the simulated hydrological response of the basin during five nonoverlapping 30-year periods from 1951 to 2099, by using the aforementioned downscaled climate model outputs of precipitation and temperature, considering or not the variability introduced by surface elevation. In particular, to filter out orographic influences from both climate model forcings, downscaled precipitation products using the parametric approach were reprojected to the mean elevation of the whole Flumendosa basin (referred to henceforth as PARnoZ) using a rainfall gradient computed through averaged precipitation values of local rain gauges versus their elevations, as in Badas et al. (2006). With the same purpose, downscaled temperature outputs were reported at the mean elevation of the basin (referred to henceforth as TnoZ) using a lapse rate (i.e., the temperature decrease per unit of elevation) estimated in Caracciolo et al. (2017) as the slope of the straight line that interpolates the observed mean annual temperature in Sardinia versus elevation. In doing so, we seek to shed light on the effects of surface elevation and spatial resolution of the statistical correction on the hydrological cycle of the basin.

Hydrologic Modeling

To simulate the hydrological response of the basin in terms of discharge, actual evapotranspiration, and leakage, we used the TOPKAPI-X, the extended version of the TOPKAPI rainfall-runoff model (Ciarapica and Todini 2002; Liu et al. 2005). This model has been successfully implemented as a research and operational hydrological model in several catchments worldwide (e.g., Bartholomes and Todini 2005; Liu et al. 2005; Martina et al. 2006). TOPKAPI-X combines basin topography with the kinematic approach, and consists of five modules that simulate the main hydrological processes including subsurface flow, overland flow, channel flow, evapotranspiration, and snowmelt, simulated at an hourly time step. Four nonlinear reservoir differential equations [obtained by combining continuity of mass and momentum equations and solved using a two-dimensional (2D) finite difference method] are used to describe subsurface flow into the soil

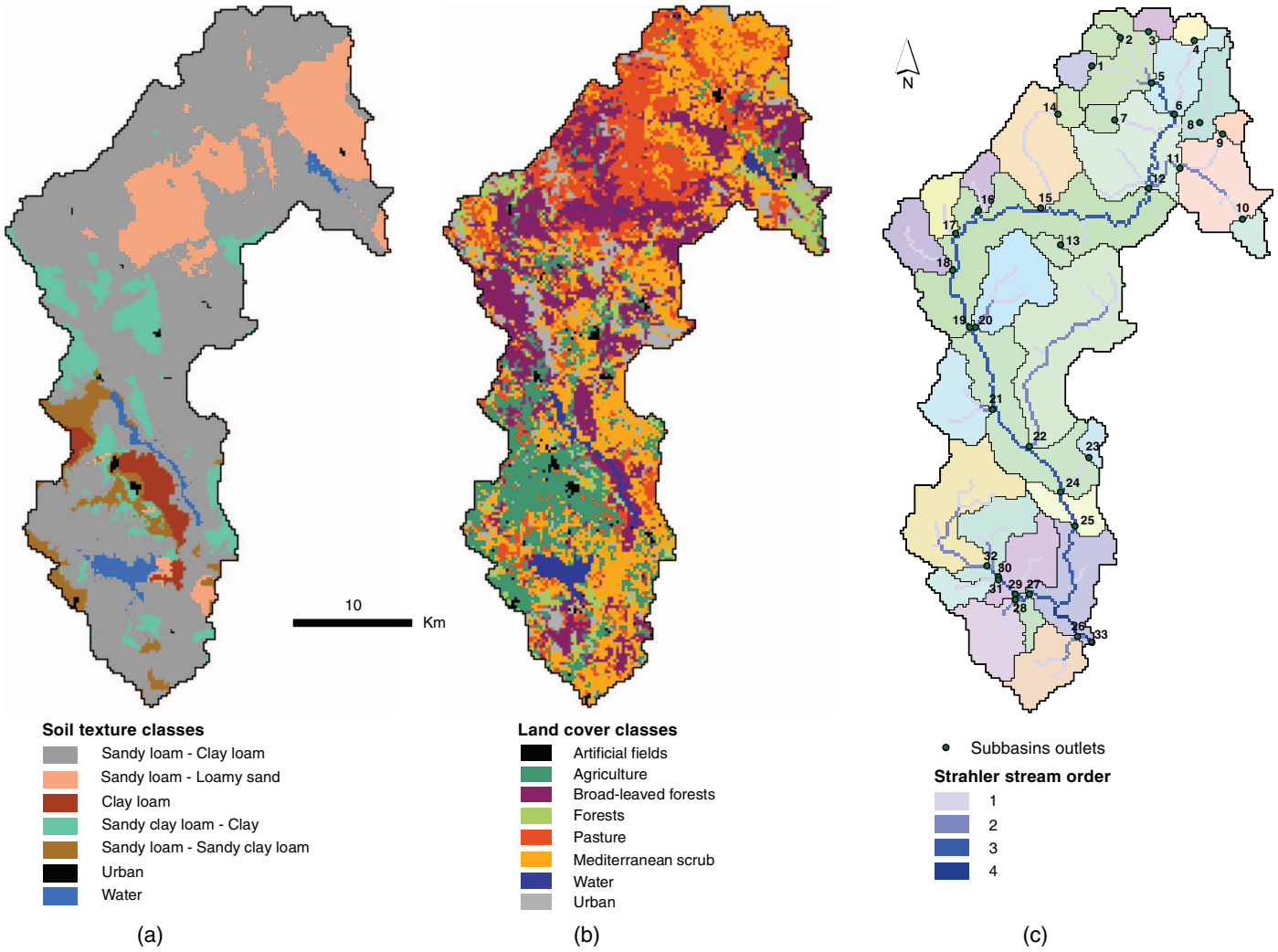

Fig. 3. (Color) (a) Soil texture; (b) land cover; and (c) subbasin maps of the Flumendosa basin.

(schematized in two layers, superficial and deep), overland flow, and channel flow. The soil module is fundamental to determine flow in unsaturated conditions. The soil zone is divided into two layers with different parameters, whose interaction allows both Dunne and Horton runoff mechanisms. The superficial layer is characterized by thin thickness and high hydraulic conductivity, and it plays a key role in direct flow contributions to the drainage network and in the activation of the saturated area, which causes surface flow (Perra et al. 2019). The deep layer is characterized by a greater thickness and reduced hydraulic conductivity, and plays a key role in determining infiltration and base flow. The model uses a regular grid to represent the terrain and it is considered suitable even for real-time flood forecasting because of its computational efficiency. Model inputs consist of spatially variable meteorological data and surface properties. For further details on the model we refer the reader to Liu and Todini (2002).

A resolution of 250 m was chosen to implement the TOPKAPI-X for the Flumendosa basin, as a compromise between computational time and accuracy. The hydrological model was calibrated to observed discharges using measured temperature and precipitation series during the period 1926–1936, and then applied in cascade with climate models using the downscaling techniques reported in the section on downscaling techniques. In particular, model calibration was performed manually using the hydrometeorological data described in the study area and dataset section before the reservoir construction during the years 1927–1931, while potential evapotranspiration (ETP) data are estimated in TOPKAPI-X using the Thornthwaite and Mather formula (Thornthwaite and Mather 1955). A spin-up interval of one year was used prior to the start of the calibration period. The available data during the period 1932–1936 were used to validate the model performance. An initial guess for the model parameters was derived from the available map of soil types [Fig. 3(a)], by assuming parameter values taken from the literature (Rawls et al. 1982). Following Ciarapica and Todini (2002) and results of a sensitivity analysis, the most influential parameters were found to be the saturated hydraulic conductivity at the surface (K_s) and the Manning coefficient (n). The values of K_s were modified within the ranges typical for the corresponding soil texture classes. For the Manning coefficient of the drainage network we assumed literature values ranging from 0.03 to 0.04 $m^{-1/3}$ s (Chow 1959), while for other parameters we adopted literature values for similar soil properties (Rawls et al. 1982). The model parameters used to characterize the three predominant soil types found within the considered basin are reported in Table 2. Because for the TOPKAPI-X model two layers are possible to discretize the soil, thickness values of 0.4 and 0.7 m were chosen for the superficial and deep layers, respectively, and for the deep layer

Table 1. Terrain, soil texture, and land cover characteristics of Flumendosa subbasins, with outlet shown in Fig. 3(c), including: contributing area (A_c), mean elevation (H_{mean}), and slope

Subbasin ID	A_c (km^2)	H_{mean} (m.a.s.l.)	Slope (%)	Soil texture classes (%)							Land cover classes (%)							
				S1	S2	S3	S4	S5	S6	S7	L1	L2	L3	L4	L5	L6	L7	L8
1	8.81	1,378	26.54	100	—	—	—	—	—	—	—	—	8	—	70	7	—	15
2	7.56	1,276	18.6	100	—	—	—	—	—	—	—	9	2	—	59	30	—	—
3	7.63	1,185	20.41	100	—	—	—	—	—	—	—	65	—	35	—	—	—	—
4	6.38	1,206	15.49	100	—	—	—	—	—	—					30	69	—	1
5	58.75	1,204	22.21	97	3	—	—	—	—	—	—	2	6	—	46	41	—	5
6	**94.94**	**1,151**	**19.36**	**82**	**18**	—	—	—	—	—	**1**	**2**	**7**	—	**40**	**47**	—	**3**
7	6.75	1,306	31.96	100	—	—	—	—	—	—	—	2	19	—	36	43	—	—
8	18.56	1,020	12.53	9	91	—	—	—	—	—	—	2	27	5	19	43	1	5
9	6.25	1,026	15.77	17	83	—	—	—	—	—	—	3	73	—	1	21	—	2
10	8.75	933	13.1	61	39	—	—	—	—	—	1	14	6	59	4	11	1	4
11	62.63	909	11.89	55	40	—	—	—	—	5	1	9	24	19	10	22	6	8
12	250.13	1,053	17.57	63	36	—	—	—	—	1	1	4	17	5	30	37	2	4
13	6.44	1,074	15.82	31	69	—	—	—	—	—	—	1	14	—	30	17	—	38
14	7.75	1,509	26.09	92	8	—	—	—	—	—	—	1	13	—	84	2	—	—
15	60.06	1,158	26.26	72	26	—	2	—	—	—	—	3	41	—	48	4	—	4
16	10.56	1,047	22.77	100	—	—	—	—	—	—	—	—	24	4	41	3	—	29
17	15.00	825	22.36	99	—	—	—	—	1	—	2	5	39	28	9	11	—	8
18	23.38	814	18.87	87	—	—	13	—	—	—	1	4	17	13	28	25	—	13
19	484.13	982	20.79	66	29	—	4	—	—	1	1	3	30	5	29	25	1	6
20	40.88	814	18.81	51	22	—	27	—	—	—	—	9	30	4	15	31	—	11
21	29.75	572	10.69	29	—	5	28	39	—	—	1	37	32	2	11	13	—	4
22	100.06	797	18.18	81	3	—	14	—	1	—	2	10	25	3	7	43	—	11
23	6.56	774	12.2	94	—	—	—	6	—	—	—	38	1	11	4	44	—	2
24	736.25	883	19.86	66	21	1	9	2	—	1	1	8	28	4	22	28	1	7
25	749.63	873	19.76	65	20	2	10	2	—	1	1	8	28	4	22	28	2	7
26	30.81	459	15.34	82	—	—	5	12	1	—	1	14	19	4	8	51	—	3
27	172.63	428	8.71	56	2	6	13	15	1	7	2	41	8	5	9	23	7	5
28	29.88	435	11.94	84	—	—	11	3	—	1	2	17	28	10	11	17	1	14
29	135.75	429	7.49	49	2	7	13	18	1	9	2	48	3	3	9	24	8	3
30	**95.31**	**457**	**7.42**	**54**	**1**	**6**	**14**	**18**	**2**	**5**	**3**	**55**	**3**	**2**	**9**	**19**	**4**	**3**
31	12.00	380	6.27	43	—	—	8	41	3	6	3	48	2	14	11	18	5	1
32	64.81	482	7.42	56	1	7	11	20	2	3	4	57	4	3	9	17	2	4
33-Outlet	**1,000.75**	**760**	**17.69**	**64**	**16**	**3**	**10**	**5**	—	**2**	**1**	**15**	**24**	**4**	**19**	**29**	**2**	**6**

Note: S1 = sandy loam—clay loam; S2 = sandy loam—loamy sand; S3 = clay loam; S4 = sandy clay loam—clay; S5 = sandy loam—sandy clay loam; S6 = urban; S7 = water; L1 = artificial fields; L2 = agriculture; L3 = broad-leaved forests; L4 = forests; L5 = pasture; L6 = Mediterranean scrub; L7 = water; and L8 = urban; m a.s.l. = metres above sea level. Representative subbasins chosen for the analysis are reported in bold font.

Table 2. Parameter values of the TOPKAPI-X model for the major soil classes found in the considered subbasins

Soil properties	Variable (unit)	Sandy loam—clay loam	Sandy clay loam—clay	Sandy loam—loamy sand
Saturated hydraulic conductivity	K_s (m/s)	1.86×10^{-4}	3.79×10^{-5}	9.53×10^{-4}
Saturated soil moisture	θ_s (–)	0.458	0.436	0.445
Residual soil moisture	θ_r (–)	0.058	0.079	0.038
Head suction	ψ_a (m)	0.159	0.267	0.087
Exponent of the horizontal flow	α	2.5	2.5	2.5

the K_s values were set one order of magnitude lower. The model performances were quantified using the Nash-Sutcliffe (NS) index (Nash and Sutcliffe 1970), evaluated on the basis of daily observed and simulated volumes, resulting in performance values of $NS = 0.79$ and $NS = 0.75$ during the calibration and validation periods, respectively. Time series of simulated and observed discharge values for the calibration and validation periods are shown in Fig. 4. In addition to the acceptable NS values, one sees that the model captures well the seasonal variability, intermittency, and recession of runoff in both periods. Some disagreements in the discharge peaks are visible, which are due to the uniform temporal disaggregation of daily rainfall depths to hourly intervals used for simulation purposes.

Results

In this section the hydrological impact of projected climate change is analyzed for the Flumendosa basin during five nonoverlapping 30-year periods (i.e., 1951–1980, 1981–2010, 2011–2040, 2041–2070, and 2071–2099), with the aim to investigate the effects of surface elevation and spatial resolution of statistical downscaling approaches.

To exemplify the settings of the different approaches considered for the statistical downscaling of precipitation forcing, Fig. 5 shows the spatial distribution of the mean annual rainfall depth (mm/year) in Sardinia referred to the 2070–2099 future period, obtained using the raw and bias-corrected products for a single climate model

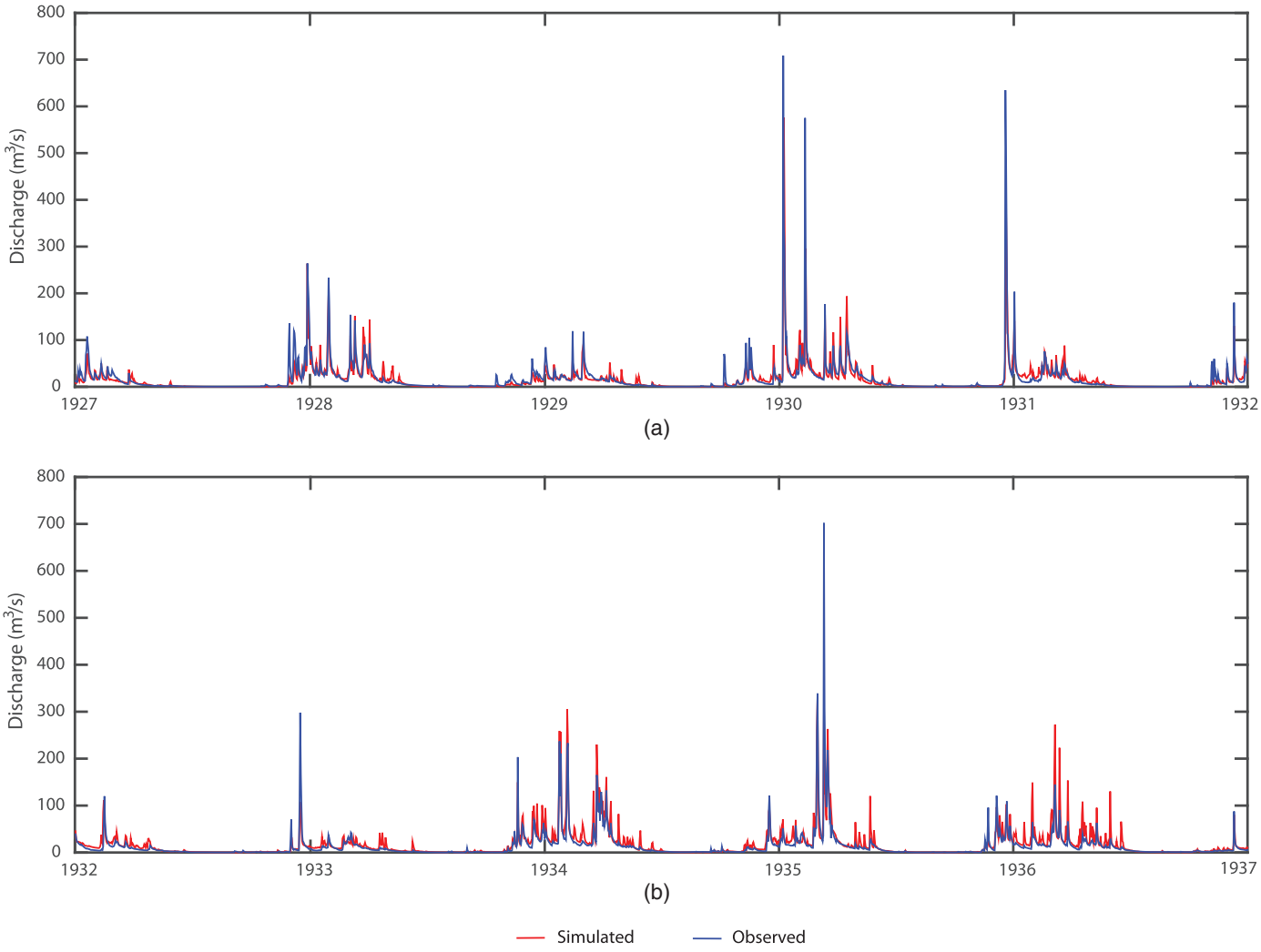

Fig. 4. (Color) Runoff simulations of the TOPKAPI-X hydrological model for Flumendosa basin during (a) calibration; and (b) validation periods.

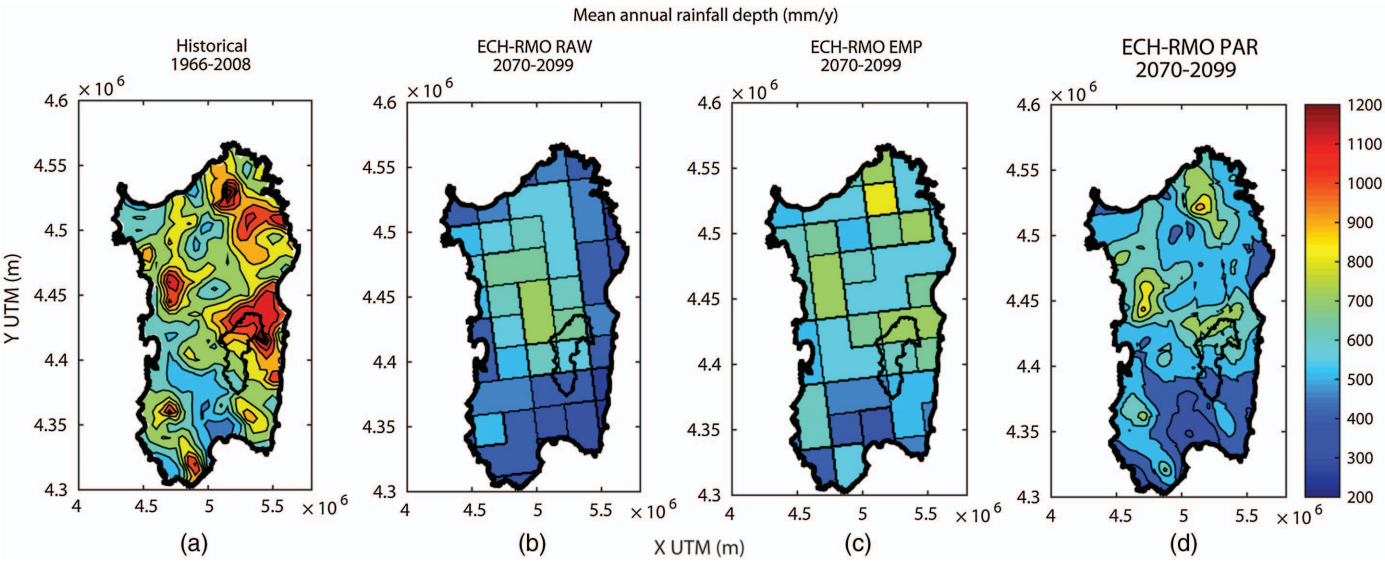

Fig. 5. (Color) Spatial distribution of the mean annual rainfall depth (mm/year) during (a) the historical period 1966–2008; and (b–d) the future period 2070–2099 simulated by climate model ECH-RMO: (b) raw climate model rainfall products (RAW); (c) bias-corrected products using empirical distribution mapping (EMP); and (d) bias-corrected products using parametric distribution mapping (PAR).

(ECH-RMO). In the same figure, the mean annual precipitation depth during the period 1966–2008 obtained using historical records of daily measurements is also reported [Fig. 5(a)], in order to make the contrast between historical and future precipitation patterns. A comparison of the historical and climate model simulated rainfall (both raw and bias-corrected) for the historical period 1966–2008 can be found in Fig. 7 of Mamalakis et al. (2017). As a general remark, one notices that the raw climate model results [Fig. 5(b)] cannot capture the spatial distribution of the mean annual rainfall. The nonparametric approach based on empirically derived Q-Q correction relationships [Fig. 5(c)] improves the results of the raw climate model, while the parametric approach allows for a more reliable representation of precipitation, considering the influence of topography. Moreover, one sees that the area with the highest precipitation depths in the high-resolution parametrically downscaled future projections [Fig. 5(d)] remains mainly the same (i.e., on the west side of the island, in the Gennargentu range) as in the historical period [Fig. 5(a)], while the mean annual precipitation depth is significantly reduced in the future. In fact, the mean annual rainfall over the island during the historical period is 780 mm/year, while in the future period it reduces to 550 mm/year.

Fig. 6 investigates the hydrological response in terms of mean annual runoff (Q) values per unit catchment area, during the five 30-year periods from 1951 to 2099, obtained using different climate precipitation forcings, namely: raw rainfall products (RAW), bias-corrected products using empirical distribution mapping (EMP), bias-corrected products using parametric distribution mapping (PAR), and bias-corrected products using parametric distribution mapping reprojected to the mean elevation of the basin (PARnoZ). Results are shown for each climate model (from the first line ECH-RCA, ECH-REM, ECH-RMO, and HCH-RCA) at the outlet of the whole Flumendosa basin (a, d, g, j) and at a representative mountainous (b, e, h, k) and valley (c, f, i, l) subbasins, among the 32 subcatchments identified in the study area and dataset section (subbasins 6 and 30 in Table 1, respectively). As a general remark, looking at all climate models results in Fig. 6, one notices that the mountainous and valley subbasins (b, e, h, k; and c, f, i, l) exhibit

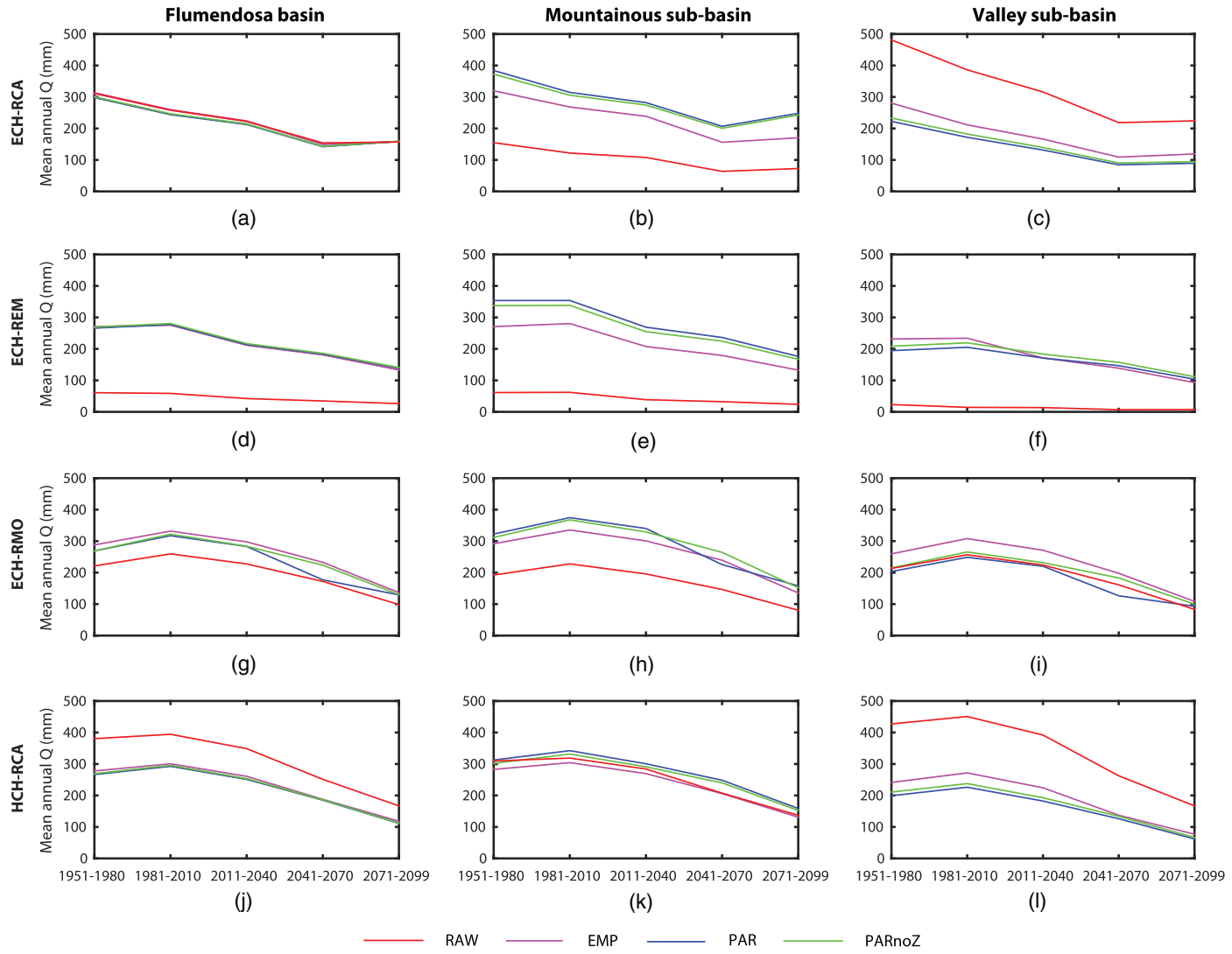

Fig. 6. (Color) Mean annual runoff (Q) values during the five nonoverlapping 30-year periods from 1951 to 2099 at the outlet Flumendosa basin (a, d, g, j), and at representative mountainous and valley subbasins (b, e, h, k; and c, f, i, l, respectively), considering the four climate models (ECH-RCA, ECH-REM, ECH-RMO, HCH-RCA) and obtained using: raw rainfall products (RAW), bias-corrected products using empirical distribution mapping (EMP), bias-corrected products using parametric distribution mapping (PAR), and bias-corrected products using parametric distribution mapping reprojected to the mean elevation of the basin (PARnoZ).

higher spread of the simulated runoff values with respect to the outlet (a, d, g, j). This is due to the fact that as the watershed area increases, the spatial and temporal integration introduced by the runoff processes becomes more influential, with subsequent reduction of the epistemic variability introduced by the different types of precipitation forcing (i.e., RAW, EMP, PAR, and PARnoZ). Another general observation is that the reduction of precipitation values in future periods results in a reduction of discharge. In addition, as noted in the discussion of Fig. 5, raw climate models exhibit large biases in simulating past and future precipitation and, therefore, the corresponding simulated discharge values in Fig. 6 (red lines) cannot be used as an adequate basis to assess the hydrological impacts of climate change.

Focusing on the effect of elevation on PAR precipitation forcing, Fig. 6 suggests that there are minimal differences between the discharge values obtained by considering (or not) orographic influences. In fact, the PAR and PARnoZ lines (blue and green, respectively) are very close to each other, independent of the climate model used, and the area and type of the subcatchment considered (i.e., mountainous subcatchment, valley subcatchment, or the whole Flumendosa basin). An exception occurs for model ECH-RMO in the period 2041–2070 where, independent of the subcatchment considered, the mean annual runoff depths obtained using PARnoZ precipitation and temperature forcings (green lines) are irregularly higher than those of the PAR case (blue lines). We have investigated this issue in some detail, and concluded that the observed deviation should be attributed to the deintensification of actual evapotranspiration, caused by the changes introduced to the simulated hydrological cycle by the rainfall and temperature reprojection process.

Focusing on the effect of spatial resolution of the considered downscaling approaches, one notices that there are important differences between the discharge values obtained using PAR (blue lines) and EMP (pink lines) as precipitation forcing to the hydrological model. This finding highlights the important effect of the spatial resolution of downscaled climate model precipitation products on hydrologic simulations.

Fig. 6 also indicates that, at the outlet of the whole Flumendosa basin, the best-performing climate model, for which all downscaling techniques apply the smallest average correction to precipitation, is ECH-RCA [i.e., the lines representing raw (red) and downscaled runoff values (other colors) are almost identical; see Fig. 6(a)]. Hence, for the sake of brevity, in what follows we focus discussion on hydrologic variables simulated for the whole Flumendosa basin and the two representative subbasins, using climate model precipitation and temperature products from ECH-RCA.

Fig. 7 shows results on the mean annual values of precipitation (P), potential ETP, actual evapotranspiration (ETA), discharge (Q), and leakage (L), for the whole Flumendosa basin and the considered mountainous and valley subbasins, during the five 30-year periods from 1951 to 2099. The results obtained using different types of precipitation input are indicated as follows: raw climate model results (RAW), bias-corrected products using empirical distribution mapping (EMP), bias-corrected products using parametric distribution mapping (PAR), and bias-corrected products using parametric distribution mapping reprojected to the mean elevation of the basin (PARnoZ). Similarly, the results obtained using downscaled temperature products, and downscaled temperature products reprojected to the mean elevation of the basin are indicated by (T) and (TnoZ), respectively. One sees that surface elevation has little influence on the mean annual values of downscaled precipitation [see blue and green lines in Figs. 7(a–c)], relative to the effects introduced by the spatial resolution of the downscaling approaches (namely 1 and 25 km for the PAR and EMP approaches, respectively). The differences are more pronounced for the valley subbasin relative to the mountainous one.

Figs. 7(d–f) illustrate how the removal of surface elevation information from the downscaled temperature climate forcing (TnoZ) affects potential evapotranspiration (ETP). One sees that, in the mountainous and valley subbasins [Figs. 7(e and f)], the corresponding values of ETP change significantly when excluding orographic influences, whereas when the whole Flumendosa basin is considered the differences are smeared out due to spatial averaging effects. In addition, at the mountainous subbasin, the ETP values are lower than those at the valley subbasin, due to the lower temperatures observed at higher altitudes. Also, note that at the mountainous (valley) subbasin the ETP values calculated when reprojecting temperature at the mean elevation of the basin (TnoZ line) are lower (higher) than those corresponding to the actual basin elevations (T line). The reason for this lies in the elevation distribution of the considered subbasins: the mountainous subbasin exhibits a right-skewed elevation distribution, while the valley subbasin distribution is left-skewed (distributions not shown). For the mountainous subbasin, this implies that during reprojection higher elevations exhibiting lower temperatures shift ETP towards higher values. The opposite holds for the valley subbasin.

As expected, results in terms of ETA show less actual evapotranspiration at the mountainous subbasin relative to the valley one [Figs. 7(h and i)]. A common feature independent of the rainfall product used (i.e., red, pink, blue, or green lines), is that filtering orographic influences out (or not) from temperature (TnoZ lines and T lines, respectively) results in effects on ETA [Figs. 7(g–i)] that are less pronounced than those on ETP [Figs. 7(d–f)]. The reason for this is the dependence of ETA on the soil moisture content, which is influenced by the amount of rainfall. The latter is not sensitive to surface elevation [see blue (PAR) and green (PARnoZ) lines in Figs. 7(a–c), and discussion above] and, therefore, for all considered cases excluding or not orographic influences from the downscaled precipitation forcing results in negligible effects on ETA [Figs. 7(g–i)]. Turning to the spatial resolution of the statistical correction method used, one sees significant differences between the ETA values obtained when using the PAR and EMP products (green and pink lines, respectively). The differences are more pronounced for the valley subbasin [Fig. 7(i)] relative to the mountainous one (Fig. 7h), following the same pattern observed in rainfall [Figs. 7(c and b)].

Regarding discharge (Q), while almost no differences can be observed at the outlet of the Flumendosa basin [Fig. 7(j)] due to the significant effect of the temporal and spatial integration applied by the runoff processes (see also discussion on Fig. 6 above), as the catchment size decreases [Figs. 7(k and l)], Q becomes increasingly sensitive to the spatial resolution of the downscaled precipitation values. As indicated in Figs. 7(k and l), the differences between the runoff values obtained using the PAR and EMP precipitation products (blue and pink lines, respectively), are much more pronounced relative to those resulting from filtering out the orographic effect from P (blue and green lines, respectively). In addition, independently of the precipitation forcing, excluding or not orographic influences from T (TnoZ and T lines, respectively) results in negligible impact on Q.

Considering L for the whole Flumendosa basin [Fig. 7(m)], one sees noticeable differences originating from precipitation products with different spatial resolutions (namely PAR and EMP, blue and pink lines, respectively), whereas elevation effects on precipitation (PAR and PARnoZ, blue and green lines, respectively) and temperature (T and TnoZ lines) affect minimally the results. For the valley subbasin [Fig. 7(o)], the observed differences between the L values originating from different precipitation and temperature products

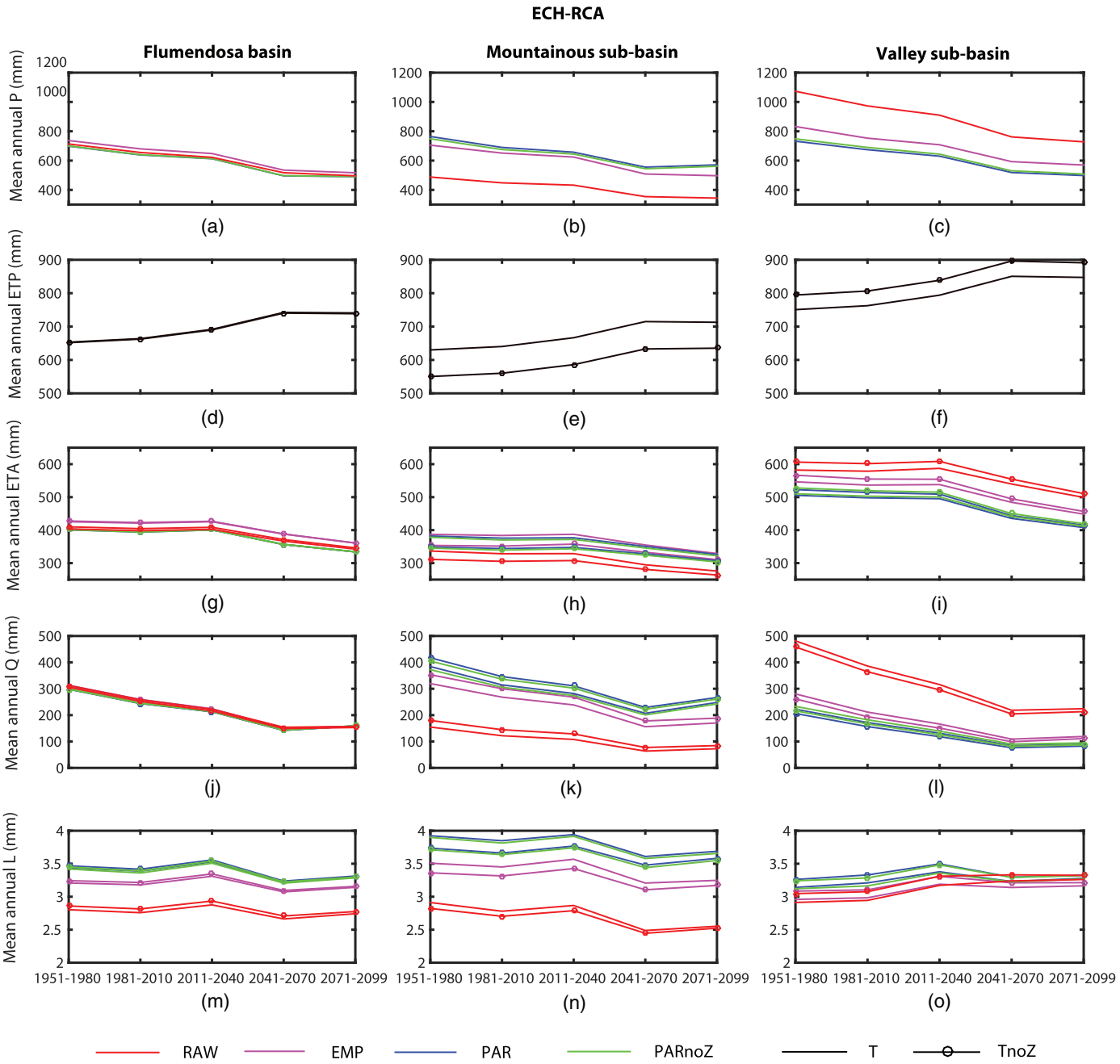

Fig. 7. (Color) Mean annual values of hydrological budget components, namely precipitation (P), potential evapotranspiration (ETP), actual evapotranspiration (ETA), discharge (Q), and leakage (L), during the five nonoverlapping 30-year periods from 1951 to 2099 for the whole Flumendosa basin, and at representative mountainous and valley subbasins, considering the ECH-RCA model and obtained using: raw rainfall products (RAW), bias-corrected products using empirical distribution mapping (EMP), bias-corrected products using parametric distribution mapping (PAR), bias-corrected products using parametric distribution mapping reprojected to the mean elevation of the basin (PARnoZ), downscaled temperature products (T), and downscaled temperature products re-projected to the mean elevation of the basin (TnoZ).

are less pronounced relative to the mountainous one [Fig. 7(n)]. An explanation for this behavior should be sought in soil moisture dynamics, because higher ETA values in valley subbasins [see above and Figs. 7(h and i)] result in lower leakage levels relative to mountainous catchments, making L less sensitive to precipitation forcing.

Fig. 8 illustrates how the mean differences of precipitation (P; a and c) and runoff (Q; b and d) in the five nonoverlapping periods considered are affected by the elevation (PAR and PARnoZ values; a and b) and spatial resolution of statistical downscaling approaches (PAR and EMP values; c and d), for all 32 subbasins considered. The results are presented in the form of scatterplots with respect to the elevation of the subbasins, for all climate models used (indicated by different colors). Regarding the influence of surface elevation on precipitation and runoff [Figs. 8(a and b), respectively], one sees that independent of the climate model used, the mean differences between PAR and PARnoZ values are close to zero at the mean elevation of Flumendosa basin [i.e., 760 metres above sea level (m a.s.l.)]. The differences become positive (negative) for subbasin elevations larger (lower) than the mean elevation of

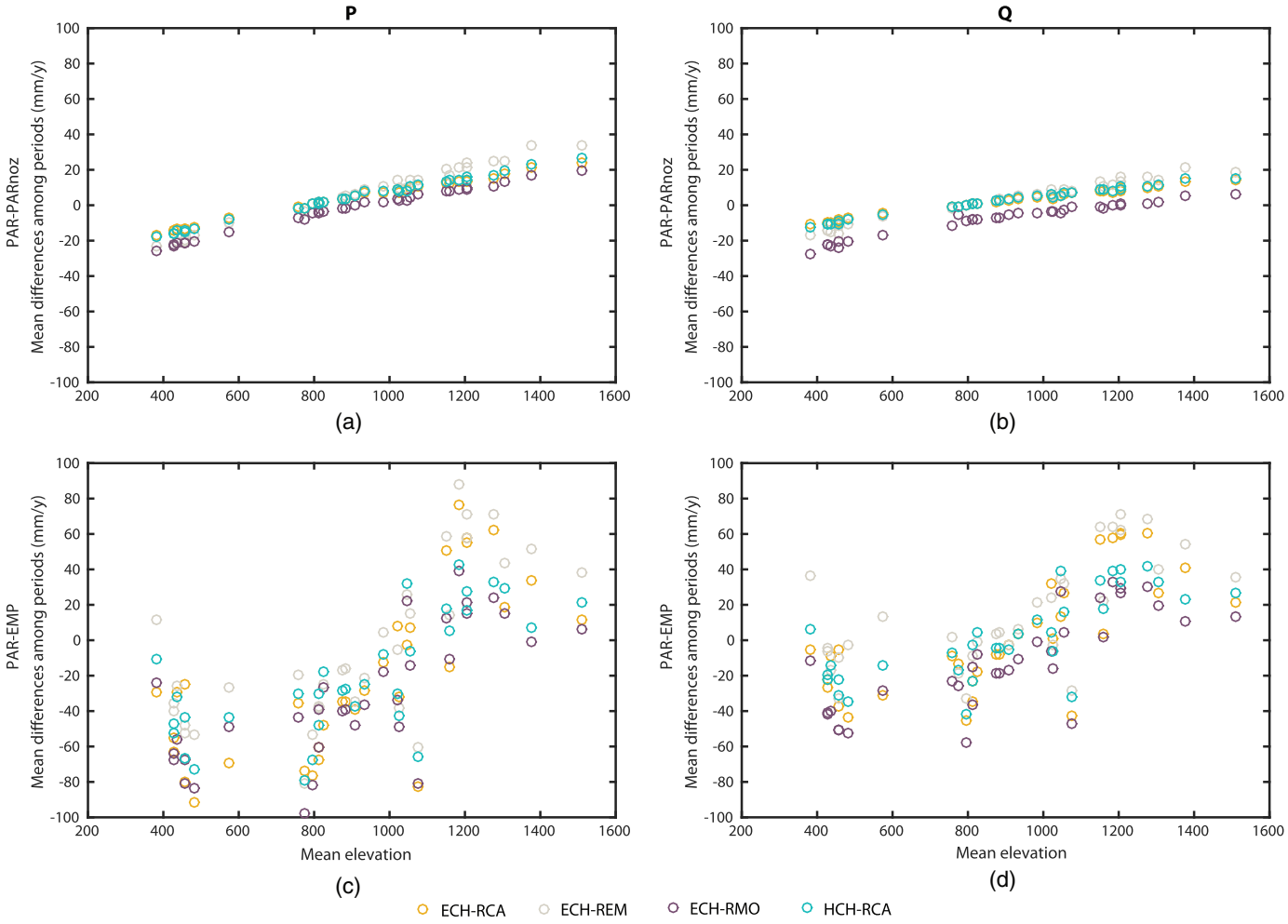

Fig. 8. (Color) Effects of the elevation, and the spatial resolution of statistical downscaling approaches on precipitation (P; a and c) and runoff (Q; b and d). Results are presented in terms of mean differences (PAR—PARnoZ, a and b; PAR—EMP, c and d) in the five nonoverlapping periods from 1951 to 2099, for the 32 subbasins in Table 1 as a function of their elevation, for all climate models used (indicated by different colors).

Flumendosa, due to the fact that parametric high-resolution downscaling (PAR) takes implicitly into account the orography. Regarding the influence of the spatial resolution of statistical downscaling approaches on precipitation and runoff [Figs. 8(c and d), respectively], one notices a wider range of variation of the mean differences between PAR and EMP estimates, relative to PAR and PARnoZ [Figs. 8(a and b)]. However, similar to Figs. 8(a and b), the mean differences cluster in the positive (negative) domain for subbasin elevations larger (lower) than the mean elevation of Flumendosa.

Conclusions

This study investigated the effects of surface elevation and spatial resolution of statistical correction methods on the hydrological cycle of a Mediterranean basin, the Flumendosa, located in Sardinia (Italy). For this aim we used four combinations of GCM/RCM historical runs and future projections, statistically downscaled using: (1) the parametric scheme of Mamalakis et al. (2017) for bias-correction and high-resolution downscaling (1 km); and (2) a nonparametric approach based on empirically derived Q-Q correction relationships, with nominal resolution equal to that of GCM/RCM results (25 km). An important advancement relative to previous studies is that we analyzed the simulated hydrological response of the basin using: (1) downscaled precipitation products from the aforementioned climate models using two statistical approaches that are conceptually equivalent but exhibit different spatial resolutions, and (2) downscaled temperature considering or not the effects of surface elevation (in the latter case by reprojecting temperature fields at the mean elevation of the Flumendosa basin). The hydrological budget of the catchment, simulated using the TOPKAPI-X model, was evaluated during five nonoverlapping 30-year periods (1951–1980, 1981–2010, 2011–2040, 2041–2070, and 2071–2099) and at multiple spatial scales (at the outlet of the Flumendosa basin and at 32 subcatchments).

The obtained findings show that, independently of the size of the considered subcatchment, the elevation factor affects only to a small degree the simulated hydrological response, while the spatial resolution of the downscaled precipitation fields has significant impact on the simulated hydrological variables and budget components. In particular, when considering the whole Flumendosa basin, the averaging effects introduced by the basin runoff processes smear out differences originating from the spatial resolution of the precipitation forcing but, as the watershed area of the subcatchments decreases, the averaging effects become less influential, with subsequent increase of the sensitivity of the simulated hydrologic response to the spatial resolution of the downscaled precipitation

values. These findings underline the importance of running hydrological models using high-resolution downscaled climate model outputs, in particular for precipitation, as high-resolution detail is of great importance for basin-scale hydrological applications and impact assessments. Indeed, the results highlight the important need to develop new and improve existing methods for bias correction and high-resolution downscaling of climate model results, because the high-resolution component is currently absent in most climate model simulations.

Data Availability Statement

Some or all data, models, or code generated or used during the study are available from the corresponding author by request.

Acknowledgments

The authors acknowledge the financial support received from the Sardinian Region, under grant L.R. 7/2007, funding call 2017, CUP: F76C18000920002, and a Ph.D. scholarship (for the first author) from the P.O.R. Sardegna F.S.E. Operational Programme of the Autonomous Region of Sardinia, European Social Fund 2007–2013—Axis IV Human Resources, Objective l.3, Line of Activity l.3.1. This work was partially supported by the Fondazione di Sardegna, funding call 2017, project: Impacts of climate change on water resources and floods, CUP: F71I17000270002. The authors would like to thank the Editor, Associate Editor, and three anonymous reviewers for their constructive comments and suggestions.

References

Aru, A., P. Baldaccini, and A. Vacca. 1992. *Carta deisuolidellaSardegna 1:250,000*. Cagliari, Italy: RegioneAutonomadellaSardegna, AssessoratoProgrammazione, BilancioedAssetto del Territorio.

Badas, M. G., R. Deidda, and E. Piga. 2006. "Modulation of homogeneous space-time rainfall cascades to account for orographic influences." *Nat. Hazards Earth Syst. Sci.* 6 (3): 427–437. https://doi.org/10.5194/nhess-6-427-2006.

Baguis, P., E. Roulin, P. Willems, and V. Ntegeka. 2010. "Climate change scenarios for precipitation and potential evapotranspiration over central Belgium." *Theor. Appl. Climatol.* 99 (3–4): 273–286. https://doi.org/10.1007/s00704-009-0146-5.

Bartholomes, J., and E. Todini. 2005. "Coupling meteorological and hydrological models for flood forecasting." *Hydrol. Earth Syst. Sci.* 9 (4): 333–346. https://doi.org/10.5194/hess-9-333-2005.

Bates, B. C., S. P. Charles, and J. P. Hughes. 1998. "Stochastic downscaling of numerical climate model simulations." *Environ. Modell. Softw.* 13 (3–4): 325–331.

Briggs, D. J., D. Martin, and . 1988. "CORINE: An environmental information system for the European Community." *Eur. Environ. Rev.* 2 (1): 29–34.

Busuioc, A., F. Giorgi, X. Bi, and M. Ionita. 2006. "Comparison of regional climate model and statistical downscaling simulations of different winter precipitation change scenarios over Romania." *Theor. Appl. Climatol.* 86 (1–4): 101–123. https://doi.org/10.1007/s00704-005-0210-8.

Cannon, A. J., S. R. Sobie, and T. Q. Murdock. 2015. "Bias correction of GCM precipitation by quantile mapping: How well do methods preserve changes in quantiles and extremes?" *J. Clim.* 28 (17): 6938–6959. https://doi.org/10.1175/JCLI-D-14-00754.1.

Caracciolo, D., R. Deidda, and F. Viola. 2017. "Analytical estimation of annual runoff distribution in ungauged seasonally dry basins based on a first order Taylor expansion of the Fu's equation." *Adv. Water Resour.* 109 (Nov): 320–332. https://doi.org/10.1016/j.advwatres.2017.09.019.

Casper, M. C., G. Grigoryan, O. Gronz, O. Gutjahr, G. Heinemann, R. Ley, and A. Rock. 2012. "Analysis of projected hydrological behavior of catchments based on signature indices." *Hydrol. Earth Syst. Sci.* 16 (2): 409–421. https://doi.org/10.5194/hess-16-409-2012.

Chang, S., W. Graham, J. Geurink, N. Wanakule, and T. Asefa. 2018. "Evaluation of impacts of future climate change and water use scenarios on regional hydrology." *Hydrol. Earth Syst. Sci.* 22: 4793–4813. https://doi.org/10.5194/hess-22-4793-2018.

Charles, S. P., B. C. Bates, P. H. Whetton, and J. P. Hughes. 1999. "Validation of downscaling models for changed climate conditions: Case study of southwestern Australia." *Clim. Res.* 12: 1–14.

Chen, H., C.-Y. Xu, and S. Guo. 2012a. "Comparison and evaluation of multiple GCMs, statistical downscaling and hydrological models in the study of climate change impacts on runoff." *J. Hydrol.* 434–435 (Apr): 36–45. https://doi.org/10.1016/j.jhydrol.2012.02.040.

Chen, J., F. P. Brissette, D. Chaumont, and M. Braun. 2013. "Finding appropriate bias correction methods in downscaling precipitation for hydrologic impact studies over North America." *Water Resour. Res.* 49 (7): 4187–4205. https://doi.org/10.1002/wrcr.20331.

Chen, J., F. P. Brissette, R. Leconte, J. Chen, F. P. Brissette, and R. Leconte. 2012b. "Coupling statistical and dynamical methods for spatial downscaling of precipitation." *Clim. Change* 114 (3–4): 509–526. https://doi.org/10.1007/s10584-012-0452-2.

Chow, V. T. 1959. *Open-channel hydraulics*. New York: McGraw-Hill.

Ciarapica, L., and E. Todini. 2002. "TOPKAPI: A model for the representation of the rainfall-runoff process at different scales." *Hydrol. Processes* 16 (2): 207–229. https://doi.org/10.1002/hyp.342.

Das, T., A. Bárdossy, E. Zehe, and Y. He. 2008. "Comparison of conceptual model performance using different representations of spatial variability." *J. Hydrol.* 356: 106–118. https://doi.org/10.1016/j.jhydrol.2008.04.008.

Deidda, R., M. Marrocu, G. Caroletti, G. Pusceddu, A. Langousis, V. Lucarini, M. Puliga, and A. Speranza. 2013. "Regional climate models' performance in representing precipitation and temperature over selected Mediterranean areas." *Hydrol. Earth Syst. Sci.* 17 (12): 5041–5059. https://doi.org/10.5194/hess-17-5041-2013.

Déqué, M. 2007. "Frequency of precipitation and temperature extremes over France in an anthropogenic scenario: Model results and statistical correction according to observed values." *Global Planet. Change* 57 (1–2): 16–26.

Dibike, Y. B., and P. Coulibaly. 2005. "Hydrologic impact of climate change in the Saguenay watershed: Comparison of downscaling methods and hydrologic models." *J. Hydrol.* 307 (1–4): 145–163. https://doi.org/10.1016/j.jhydrol.2004.10.012.

Dibike, Y. B., P. Gachon, A. St-Hilaire, T. B. M J Ouarda, and T-V Nguyen. 2008. "Uncertainty analysis of statistically downscaled temperature and precipitation regimes in Northern Canada." *Theor. Appl. Climatol.* 91 (1–4): 149–170. https://doi.org/10.1007/s00704-007-0299-z.

Durman, C. F., J. M. Gregory, D. C. Hassell, R. G. Jones, and J. M. Murphy. 2001. "A comparison of extreme European daily precipitation simulated by a global and a regional model for present and future climates." *Q. J. R. Meteorol. Soc.* 127 (573): 1005–1015. https://doi.org/10.1002/qj.49712757316.

Fang, G. H., J. Yang, Y. N. Chen, and C. Zammit. 2015. "Comparing bias correction methods in downscaling meteorological variables for a hydrologic impact study in an arid area in China." *Hydrol. Earth Syst. Sci.* 19 (6): 2547–2559. https://doi.org/10.5194/hess-19-2547-2015.

Fowler, H. J., S. Blenkinsop, and C. Tebaldi. 2007. "Linking climate change modelling to impacts studies: Recent advances in downscaling techniques for hydrological modelling." *Int. J. Climatol.* 27 (12): 1547–1578. https://doi.org/10.1002/joc.1556.

Fowler, H. J., and C. G. Kilsby. 2007. "Using regional climate model data to simulate historical and future river flows in northwest England." *Clim. Change* 80 (3–4): 337–367. https://doi.org/10.1007/s10584-006-9117-3.

Gagnon, P., and A. N. Rousseau. 2014. "Stochastic spatial disaggregation of extreme precipitation to validate a regional climate model and to evaluate climate change impacts over a small watershed." *Hydrol. Earth Syst. Sci.* 18 (5): 1695–1704. https://doi.org/10.5194/hess-18-1695-2014.

Giorgi, F., B. Hewitson, J. Christensen, C. Fu, R. Jones, M. Hulme, L. Mearns, H. Von Storch, and P. Whetton. 2001. "Regional climate information—Evaluation and projections." In *Proc., Climate Change 2001: The Scientific Basis*, edited by Houghton, J. T., et al., 583–638. New York: Cambridge University Press.

Gutiérrez, J. M., et al. 2018. "An intercomparison of a large ensemble of statistical downscaling methods over Europe: Results from the VALUE perfect predictor cross-validation experiment." *Int. J. Climatol.* 39 (9): 3750–3785.

Gutmann, E., T. Pruitt, M. P. Clark, L. Brekke, J. R. Arnold, D. A. Raff, and R. M. Rasmussen. 2014. "An intercomparison of statistical downscaling methods used for water resource assessments in the United States." *Water Resour. Res.* 50 (9): 7167–7186. https://doi.org/10.1002/2014WR015559.

Guyennon, N., E. Romano, I. Portoghese, F. Salerno, S. Calmanti, A. B. Petrangeli, G. Tartari, and D. Copetti. 2013. "Benefits from using combined dynamical-statistical downscaling approaches—Lessons from a case study in the Mediterranean region." *Hydrol. Earth Syst. Sci.* 17 (2): 705–720. https://doi.org/10.5194/hess-17-705-2013.

Haddeland, I., B. V. Matheussen, and D. P. Lettenmaier. 2002. "Influence of spatial resolution on simulated streamflow in a macroscale hydrologic model." *Water Resour. Res.* 38 (7): 29-1–29–10. https://doi.org/10.1029/2001WR000854.

Hagemann, S., et al. 2013. "Climate change impact on available water resources obtained using multiple global climate and hydrology models." *Earth Syst. Dyn.* 4 (1): 129–144. https://doi.org/10.5194/esd-4-129-2013.

Hasson, S., V. Lucarini, and S. Pascale. 2013. "Hydrological cycle over South and Southeast Asian river basins as simulated by PCMDI/CMIP3 experiments." *Earth Syst. Dyn.* 4 (2): 199–217. https://doi.org/10.5194/esd-4-199-2013.

Haylock, M. R., N. Hofstra, A. M. G. Klein Tank, E. J. Klok, P. D. Jones, and M. New. 2008. "A European daily high-resolution gridded data set of surface temperature and precipitation for 1950–2006." *J. Geophys. Res.* 113 (20). https://doi.org/10.1029/2008JD010201.

Hertig, E., and J. Jacobeit. 2008. "Assessments of Mediterranean precipitation changes for the 21st century using statistical downscaling techniques." *Int. J. Climatol.* 28 (8): 1025–1045. https://doi.org/10.1002/joc.1597.

Hewitson, B. C., and R. G. Crane. 1996. "Climate downscaling: Techniques and application." *Clim. Res.* 7 (2): 85–95. https://doi.org/10.3354/cr007085.

Hewitt, C. D., and D. J. Griggs. 2004. "Ensembles-based predictions of climate changes and their impacts." *Eos* 85: 566.

IPCC (The Intergovernmental Panel on Climate Change). 2014. "Climate change: Impacts, adaptation, and vulnerability. Part A: Global and sectoral aspects." In *Proc., Contribution of Working Group II to the Fifth Assessment Report of the Intergovernmental Panel on Climate Change*, edited by C. B. Field, et al. Cambridge, UK: Cambridge Univ. Press.

Jacobeit, J., E. Hertig, S. Seubert, and K. Lutz. 2014. "Statistical downscaling for climate change projections in the Mediterranean region: Methods and results." *Reg. Environ. Change* 14 (5): 1891–1906. https://doi.org/10.1007/s10113-014-0605-0.

Kaleris, V., A. Langousis, M. C. Acreman, and S. Huang. 2017. "Comparison of two rainfall-runoff models: Effects of conceptualization on water budget components." *Hydrol. Sci. J.* 62 (5): 729–748. https://doi.org/10.1080/02626667.2016.1250899.

Kiktev, D., J. Caesar, L. V. Alexander, H. Shiogama, and M. Collier. 2007. "Comparison of observed and multimodeled trends in annual extremes of temperature and precipitation." *Geophys. Res. Lett.* 34 (10): 1–5. https://doi.org/10.1029/2007GL029539.

Kjellström, E., F. Boberg, M. Castro, J. Christensen, G. Nikulin, and E. Sánchez. 2010. "Daily and monthly temperature and precipitation statistics as performance indicators for regional climate models." *Clim. Res.* 44 (2–3): 135–150. https://doi.org/10.3354/cr00932.

Kleinn, J., C. Frei, J. Gurtz, D. Lüthi, P. L. Vidale, and C. Schär. 2005. "Hydrologic simulations in the Rhine basin driven by a regional climate model." *J. Geophys. Res. D: Atmos.* 110 (4): 1–18. https://doi.org/10.1029/2004JD005143.

Langousis, A., R. Deidda, A. A. Carsteanu, C. Onof, P. Burlando, R. Uijlenhoet, and A. Bárdossy. 2018. "Precipitation measurement and modelling: Uncertainty, variability, observations, ensemble simulation and downscaling." *J. Hydrol.* 556 (Jan): 824–826. https://doi.org/10.1016/j.jhydrol.2017.09.016.

Langousis, A., and V. Kaleris. 2014. "Statistical framework to simulate daily rainfall series conditional on upper-air predictor variables." *Water Resour. Res.* 50 (5): 3907–3932. https://doi.org/10.1002/2013WR014936.

Langousis, A., A. Mamalakis, R. Deidda, and M. Marrocu. 2016. "Assessing the relative effectiveness of statistical downscaling and distribution mapping in reproducing rainfall statistics based on climate model results." *Water Resour. Res.* 52 (1): 471–494. https://doi.org/10.1002/2015WR017556.

Leander, R., T. Adri Buishand, B. J. J. M. Van Den Hurk, and M. J. M. De Wit. 2008. "Estimated changes in flood quantiles of the river Meuse from resampling of regional climate model output." *J. Hydrol.* 351 (3–4): 331–343. https://doi.org/10.1016/j.jhydrol.2007.12.020.

Leander, R., and T. A. Buishand. 2007. "Resampling of regional climate model output for the simulation of extreme river flows." *J. Hydrol.* 332 (3–4): 487–496. https://doi.org/10.1016/j.jhydrol.2006.08.006.

Lenderink, G., A. Buishand, and W. Van Deursen. 2007. "Estimates of future discharges of the river Rhine using two scenario methodologies: Direct versus delta approach." *Hydrol. Earth Syst. Sci.* 11 (3): 1145–1159. https://doi.org/10.5194/hess-11-1145-2007.

Liu, Z., M. L. V. Martina, and E. Todini. 2005. "Flood forecasting using a fully distributed model: Application of the TOPKAPI model to the Upper Xixian Catchment." *Hydrol. Earth Syst. Sci.* 9 (4): 347–364. https://doi.org/10.5194/hess-9-347-2005.

Liu, Z., and E. Todini. 2002. "Towards a comprehensive physically-based rainfall-runoff model." *Hydrol. Earth Syst. Sci.* 6 (5): 859–881. https://doi.org/10.5194/hess-6-859-2002.

Ludwig, R., et al. 2010. "Climate-induced changes on the hydrology of mediterranean basins—A research concept to reduce uncertainty and quantify risk." *Fresenius Environ. Bull.* 19 (10A): 2379–2384.

Lutz, K., J. Jacobeit, A. Philipp, S. Seubert, H. Kunstmann, and P. Laux. 2012. "Comparison and evaluation of statistical downscaling techniques for station-based precipitation in the Middle East." *Int. J. Climatol.* 32 (10): 1579–1595. https://doi.org/10.1002/joc.2381.

Mamalakis, A., A. Langousis, R. Deidda, and M. Marrocu. 2017. "A parametric approach for simultaneous bias correction and high-resolution downscaling of climate model rainfall." *Water Resour. Res.* 53 (3): 2149–2170. https://doi.org/10.1002/2016WR019578.

Mao, G., S. Vogl, P. Laux, S. Wagner, and H. Kunstmann. 2015. "Stochastic bias correction of dynamically downscaled precipitation fields for Germany through Copula-based integration of gridded observation data." *Hydrol. Earth Syst. Sci.* 19 (4): 1787–1806. https://doi.org/10.5194/hess-19-1787-2015.

Maraun, D., et al. 2010. "Precipitation downscaling under climate change: Recent developments to bridge the gap between dynamical models and the end user." *Rev. Geophys.* 48 (3): 1–34. https://doi.org/10.1029/2009RG000314.

Martina, M. L. V., E. Todini, and A. Libralon. 2006. "Rainfall thresholds for flood warning systems: A Bayesian decision approach." In *Hydrological modelling and the water cycle*, 203–227. Berlin: Springer.

Maurer, E. P., and H. G. Hidalgo. 2008. "Utility of daily vs. monthly large-scale climate data: An intercomparison of two statistical downscaling methods." *Hydrol. Earth Syst. Sci.* 12 (2): 551–563. https://doi.org/10.5194/hess-12-551-2008.

Mearns, L. O., F. Giorgi, L. McDaniel, and C. Shields. 1995. "Analysis of daily variability of precipitation in a nested regional climate model: Comparison with observations and doubled CO_2 results." *Global Planet. Change* 10 (1–4): 55–78. https://doi.org/10.1016/0921-8181(94)00020-E.

Mearns, L. O., F. Giorgi, P. Whetton, D. Pabon, M. Hulme, and M. Lal. 2003. "Guidelines for use of climate scenarios developed from regional climate model experiments." *IPCC Guidelines* 38: 1–38.

Mehrotra, R., A. Sharma, R. Mehrotra, and A. Sharma. 2016. "A multivariate quantile-matching bias correction approach with auto- and cross-dependence across multiple time scales: Implications for downscaling." *J. Clim.* 29 (10): 3519–3539. https://doi.org/10.1175/JCLI-D-15-0356.1.

Mendoza, P. A., M. P. Clark, N. Mizukami, A. J. Newman, M. Barlage, E. D. Gutmann, R. M. Rasmussen, B. Rajagopalan, L. D. Brekke, and J. R. Arnold. 2014. "Effects of hydrologic model choice and calibration on the portrayal of climate change impacts." *J. Hydrometeorol.* 16 (2): 762–780. https://doi.org/10.1175/JHM-D-14-0104.1.

Michelangeli, P. A., M. Vrac, and H. Loukos. 2009. "Probabilistic downscaling approaches: Application to wind cumulative distribution functions." *Geophys. Res. Lett.* 36 (11): 1–6. https://doi.org/10.1029/2009GL038401.

Nash, J. E., and J. V. Sutcliffe. 1970. "River flow forecasting through conceptual models. Part I: A discussion of principles." *J. Hydrol.* 10 (3): 282–290. https://doi.org/10.1016/0022-1694(70)90255-6.

Nover, D. M., J. W. Witt, J. B. Butcher, T. E. Johnson, and C. P. Weaver. 2016. "The effects of downscaling method on the variability of simulated watershed response to climate change in five U.S. Basins." *Earth Interact* 20: 1–26. https://doi.org/10.1175/EI-D-15-0024.s1.

Ochoa, A., L. Campozano, E. Sánchez, R. Gualán, and E. Samaniego. 2016. "Evaluation of downscaled estimates of monthly temperature and precipitation for a Southern Ecuador case study." *Int. J. Climatol.* 36 (3): 1244–1255. https://doi.org/10.1002/joc.4418.

Palatella, L., M. M. Miglietta, P. Paradisi, and P. Lionello. 2010. "Climate change assessment for Mediterranean agricultural areas by statistical downscaling." *Nat. Hazards Earth Syst. Sci.* 10 (7): 1647–1661. https://doi.org/10.5194/nhess-10-1647-2010.

Perra, E. 2018. "A comparative assessment of hydrologic models of varying complexity applied to a Semi—Arid Region (Sardinia, Italy) for climate change studies." Ph.D. thesis, Univ. of Cagliari, Université du Québec, Institut National de la recherche scientifique.

Perra, E., M. Piras, R. Deidda, G. Mascaro, and C. Paniconi. 2019. "Investigating parameter transferability acrossmodels and events for a semiaridmediterranean catchment." *Water* 11: 2261. https://doi.org/10.3390/w11112261.

Perra, E., M. Piras, R. Deidda, C. Paniconi, G. Mascaro, E. R. Vivoni, P. Cau, P. A. Marras, R. Ludwig, and S. Meyer. 2018. "Multimodel assessment of climate change-induced hydrologic impacts for a Mediterranean catchment." *Hydrol. Earth Syst. Sci.* 22: 4125–4143. https://doi.org/10.5194/hess-22-4125-2018.

Piani, C., J. O. Haerter, and E. Coppola. 2010. "Statistical bias correction for daily precipitation in regional climate models over Europe." *Theor. Appl. Climatol.* 99 (1–2): 187–192. https://doi.org/10.1007/s00704-009-0134-9.

Potter, N. J., M. Ekström, F. H. S. Chiew, L. Zhang, and G. Fu. 2018. "Change-signal impacts in downscaled data and its influence on hydroclimate projections." *J. Hydrol.* 564 (Sep): 12–25. https://doi.org/10.1016/j.jhydrol.2018.06.018.

Prudhomme, C., N. Reynard, and S. Crooks. 2002. "Downscaling of global climate models for flood frequency analysis: Where are we now?" *Hydrol. Processes* 16 (6): 1137–1150. https://doi.org/10.1002/hyp.1054.

Raje, D., and P. P. Mujumdar. 2009. "A conditional random field-based downscaling method for assessment of climate change impact on multisite daily precipitation in the Mahanadi basin." *Water Resour. Res.* 45 (10): 10404. https://doi.org/10.1029/2008WR007487.

Rawls, W. J., D. L. Brakensiek, K. E. Saxton. 1982. "Estimation of soil properties." *Trans. ASAE* 25 (5): 1316–1328.

Reshmidevi, T. V., D. Nagesh Kumar, R. Mehrotra, and A. Sharma. 2018. "Estimation of the climate change impact on a catchment water balance using an ensemble of GCMs." *J. Hydrol.* 556: 1192–1204. https://doi.org/10.1016/j.jhydrol.2017.02.016.

Rojas, R., L. Feyen, A. Dosio, and D. Bavera. 2011. "Improving pan-European hydrological simulation of extreme events through statistical bias correction of RCM-driven climate simulations." *Hydrol. Earth Syst. Sci.* 15 (8): 2599–2620. https://doi.org/10.5194/hess-15-2599-2011.

Rummukainen, M. 2010. "State-of-the-art with regional climate models." *Wiley Interdiscip. Rev. Clim. Change* 1 (1): 82–96. https://doi.org/10.1002/wcc.8.

Salathé, E. P. 2003. "Comparison of various precipitation downscaling methods for the simulation of streamflow in a rainshadow river basin." *Int. J. Climatol.* 23 (8): 887–901. https://doi.org/10.1002/joc.922.

Sarr, M. A., O. Seidou, Y. Tramblay, and S. El Adlouni. 2015. "Comparison of downscaling methods for mean and extreme precipitation in Senegal." *J. Hydrol. Reg. Stud.* 4: 369–385. https://doi.org/10.1016/j.ejrh.2015.06.005.

Schepen, A., Q. J. Wang, and D. E. Robertson. 2012. "Combining the strengths of statistical and dynamical modeling approaches for forecasting Australian seasonal rainfall." *J. Geophys. Res. Atmos.* 117 (D20): 1–9. https://doi.org/10.1029/2012JD018011.

Schmidli, J., C. M. Goodess, C. Frei, M. R. Haylock, Y. Hundecha, J. Ribalaygua, and T. Schmith. 2007. "Statistical and dynamical downscaling of precipitation: An evaluation and comparison of scenarios for the European Alps." *J. Geophys. Res.* 112 (D4): 4105. https://doi.org/10.1029/2005JD007026.

Seguí, P. Q., A. Ribes, E. Martin, F. Habets, and J. Boé. 2010. "Comparison of three downscaling methods in simulating the impact of climate change on the hydrology of Mediterranean basins." *J. Hydrol.* 383 (1–2): 111–124. https://doi.org/10.1016/j.jhydrol.2009.09.050.

Sennikovs, J., and U. Bethers. 2009. "Statistical downscaling method of regional climate model results for hydrological modelling." In *Proc., 18th World IMACS/MODSIM Congress*, 3962–3968. Plantation, FL: Modelling and Simulation Society of Australia and New Zealand and International Association for Mathematics and Computers in Simulation.

Smiatek, G., H. Kunstmann, R. Knoche, and A. Marx. 2009. "Precipitation and temperature statistics in high-resolution regional climate models: Evaluation for the European Alps." *J. Geophys. Res.* 114: 1–16. https://doi.org/10.1029/2008JD011353.

Smith, M. B., V. I. Koren, Z. Zhang, S. M. Reed, J. J. Pan, and F. Moreda. 2004. "Runoff response to spatial variability in precipitation: An analysis of observed data." *J. Hydrol.* 298 (1–4): 267–286. https://doi.org/10.1016/j.jhydrol.2004.03.039.

Stahl, K., L. M. Tallaksen, L. Gudmundsson, and J. H. Christensen. 2011. "Streamflow data from small basins: A challenging test to high-resolution regional climate modeling." *J. Hydrometeorol.* 12 (5): 900–912. https://doi.org/10.1175/2011JHM1356.1.

Stoll, S., H. J. Hendricks Franssen, M. Butts, and W. Kinzelbach. 2011. "Analysis of the impact of climate change on groundwater related hydrological fluxes: A multi-model approach including different downscaling methods." *Hydrol. Earth Syst. Sci.* 15 (1): 21–38. https://doi.org/10.5194/hess-15-21-2011.

Sulis, M., C. Paniconi, M. Marrocu, D. Huard, and D. Chaumont. 2012. "Hydrologic response to multimodel climate output using a physically based model of groundwater/surface water interactions." *Water Resour. Res.* 48 (12): 1–18. https://doi.org/10.1029/2012WR012304.

Sulis, M., C. Paniconi, C. Rivard, R. Harvey, and D. Chaumont. 2011. "Assessment of climate change impacts at the catchment scale with a detailed hydrological model of surface-subsurface interactions and comparison with a land surface model." *Water Resour. Res.* 47 (1): 1–22. https://doi.org/10.1029/2010WR009167.

Sun, F., M. L. Roderick, W. H. Lim, and G. D. Farquhar. 2011. "Hydroclimatic projections for the Murray-Darling Basin based on an ensemble derived from Intergovernmental Panel on Climate Change AR4 climate models." *Water Resour. Res.* 47 (4): 0–2. https://doi.org/10.1029/2010WR009829.

Sunyer, M. A., et al. 2015. "Inter-comparison of statistical downscaling methods for projection of extreme precipitation in Europe." *Hydrol. Earth Syst. Sci.* 19 (4): 1827–1847. https://doi.org/10.5194/hess-19-1827-2015.

Teutschbein, C., T. Grabs, R. H. Karlsen, H. Laudon, and K. Bishop. 2015. "Hydrological response to changing climate conditions: Spatial streamflow variability in the boreal region." *Water Resour. Res.* 51 (12): 9425–9446. https://doi.org/10.1002/2015WR017337.

Teutschbein, C., and J. Seibert. 2012. "Bias correction of regional climate model simulations for hydrological climate-change impact studies: Review and evaluation of different methods." *J. Hydrol.* 456–457 (Aug): 12–29. https://doi.org/10.1016/j.jhydrol.2012.05.052.

Teutschbein, C., and J. Seibert. 2013. "Is bias correction of regional climate model (RCM) simulations possible for non-stationary conditions." *Hydrol. Earth Syst. Sci.* 17 (12): 5061–5077. https://doi.org/10.5194/hess-17-5061-2013.

Teutschbein, C., F. Wetterhall, and J. Seibert. 2011. "Evaluation of different downscaling techniques for hydrological climate-change impact studies at the catchment scale." *Clim. Dyn.* 37 (9–10): 2087–2105. https://doi.org/10.1007/s00382-010-0979-8.

Themeßl, M. J., A. Gobiet, and A. Leuprecht. 2011. "Empirical-statistical downscaling and error correction of daily precipitation from regional climate models." *Int. J. Climatol.* 31 (10): 1530–1544. https://doi.org/10.1002/joc.2168.

Thornthwaite, C. W., and J. R. Mather. 1955. "The water balance." *Climatology* 8 (l): 5–86.

Tryhorn, L., and A. DeGaetano. 2011. "A comparison of techniques for downscaling extreme precipitation over the Northeastern United States." *Int. J. Climatol.* 31 (13): 1975–1989. https://doi.org/10.1002/joc.2208.

Urrutia, R., and M. Vuille. 2009. "Climate change projections for the tropical Andes using a regional climate model: Temperature and precipitation simulations for the end of the 21st century." *J. Geophys. Res.* 114: 2108. https://doi.org/10.1029/2008JD011021.

Van Pelt, S. C., J. J. Beersma, T. A. Buishand, B. J. J. M. Van Den Hurk, and P. Kabat. 2012. "Future changes in extreme precipitation in the rhine basin based on global and regional climate model simulations." *Hydrol. Earth Syst. Sci.* 16 (12): 4517–4530. https://doi.org/10.5194/hess-16-4517-2012.

von Storch H., E. Zorita, and U. Cubasch. 1993. "Downscaling of global climate change estimates to regional scales: An application to Iberian rainfall in wintertime." *Am. Meteorol. Soc.* 6 (6): 1161–1171.

Vrac, M., P. Drobinski, A. Merlo, M. Herrmann, C. Lavaysse, L. Li, and S. Somot. 2012. "Dynamical and statistical downscaling of the French Mediterranean climate: Uncertainty assessment." *Nat. Hazards Earth Syst. Sci.* 12 (9): 2769–2784. https://doi.org/10.5194/nhess-12-2769-2012.

Vrac, M., P. Marbaix, D. Paillard, and P. Naveau. 2007. "Climate of the Past Non-linear statistical downscaling of present and LGM precipitation and temperatures over Europe." *Clim. Past* 3: 669–682. https://doi.org/10.5194/cp-3-669-2007.

Walsh, K., and J. L. McGregor. 1995. "January and July climate simulations over the Australian region using a limited-area model." *J. Clim.* 8 (10): 2387–2403. https://doi.org/10.1175/1520-0442(1995)008<2387:JAJCSO>2.0.CO;2.

Wetterhall, F., A. Bárdossy, D. Chen, S. Halldin, and C.-Y. Xu. 2009. "Statistical downscaling of daily precipitation over Sweden using GCM output." *Theor. Appl. Climatol* 96: 95–103. https://doi.org/10.1007/s00704-008-0038-0.

Wilby, R. L. 2010. "Evaluating climate model outputs for hydrological applications." *Hydrol. Sci. J.* 55 (7): 1090–1093. https://doi.org/10.1080/02626667.2010.513212.

Wilby, R. L., S. P. Charles, E. Zorita, B. Timbal, P. Whetton, and L. O. Mearns. 2004. "Guidelines for use of climate scenarios developed from statistical downscaling methods." In *Guidance on the development of regional climate scenarios for vulnerability and adaptation assessments* 1–27. Geneva, Switzerland: Intergovernmental Panel on Climate Change.

Wilby, R. L., L. E. Hay, W. J. Gutowski, R. W. Arritt, E. S. Tackle, G. H. Leavesley, and M. Clark. 2000. "Hydrological responses to dynamically and statistically downscaled general cirulation model output." *Geophys. Res. Lett.* 27 (8): 1199–1202. https://doi.org/10.1029/1999GL006078.

Wilby, R. L., L. E. Hay, and G. H. Leavesley. 1999. "A comparison of downscaled and raw GCM output: Implications for climate change scenarios in the San Juan River basin, Colorado." *J. Hydrol.* 225 (1–2): 67–91. https://doi.org/10.1016/S0022-1694(99)00136-5.

Wilby, R. L., T. M. L. Wigley, D. Conway, P. D. Jones, B. C. Hewitson, J. Main, and D. S. Wilks. 1998. "Statistical downscaling of general circulation model output: A comparison of methods." *Water Resour. Res.* 34 (11): 2995–3008. https://doi.org/10.1029/98WR02577.

Willems, P., K. Arnbjerg-Nielsen, J. Olsson, and V. T. V. Nguyen. 2012. "Climate change impact assessment on urban rainfall extremes and urban drainage: Methods and shortcomings." *Atmos. Res.* 103 (Jan): 106–118. https://doi.org/10.1016/j.atmosres.2011.04.003.

Willems, P., and M. Vrac. 2011. "Statistical precipitation downscaling for small-scale hydrological impact investigations of climate change." *J. Hydrol.* 402 (3–4): 193–205. https://doi.org/10.1016/j.jhydrol.2011.02.030.

Wood, A. W., L. R. Leung, V. Sridhar, and D. P. Lettenmaier. 2004. "Hydrologic implications of dynamical and statistical approaches to downscaling climate model outputs." *Clim. Change* 62 (1–3): 189–216. https://doi.org/10.1023/B:CLIM.0000013685.99609.9e.

Wood, A. W., E. P. Maurer, A. Kumar, and D. P. Lettenmaier. 2002. "Long-range experimental hydrologic forecasting for the eastern United States." *J. Geophys. Res.* 107 (D20): 4429. https://doi.org/10.1029/2001JD000659.

Yoon, J. H., L. Ruby Leung, and J. Correia. 2012. "Comparison of dynamically and statistically downscaled seasonal climate forecasts for the cold season over the United States." *J. Geophys. Res. Atmos.* 117 (21): 21109. https://doi.org/10.1029/2012JD017650.

Zehe, E., R. Becker, A. Bárdossy, and E. Plate. 2005. "Uncertainty of simulated catchment runoff response in the presence of threshold processes: Role of initial soil moisture and precipitation." *J. Hydrol.* 315 (1–4): 183–202. https://doi.org/10.1016/j.jhydrol.2005.03.038.

Zorita, E., and H. von Storch. 1997. *A survey of statistical downscaling techniques*. GKSS Rep. Postfach, Geesthacht: GKSS-Forschungszentrum Geesthacht GmbH.